Allometric relationships between traveltime channel networks, convex hulls, and convexity measures

Lea Tien Tay,[1] B. S. Daya Sagar,[2] and Hean Teik Chuah[1]

Received 7 March 2005; revised 5 October 2005; accepted 24 February 2006; published 14 June 2006.

[1] The channel network (S) is a nonconvex set, while its basin [$C(S)$] is convex. We remove open-end points of the channel connectivity network iteratively to generate a traveltime sequence of networks (S_n). The convex hulls of these traveltime networks provide an interesting topological quantity, which has not been noted thus far. We compute lengths of shrinking traveltime networks $L(S_n)$ and areas of corresponding convex hulls $C(S_n)$, the ratios of which provide convexity measures $CM(S_n)$ of traveltime networks. A statistically significant scaling relationship is found for a model network in the form $L(S_n) \sim A[C(S_n)]^{0.57}$. From the plots of the lengths of these traveltime networks and the areas of their corresponding convex hulls as functions of convexity measures, new power law relations are derived. Such relations for a model network are $CM(S_n) \sim \frac{1}{L(S_n)^{0.7}}$ and $CM(S_n) \sim \frac{1}{A[C(S_n)]^{0.43}}$. In addition to the model study, these relations for networks derived from seven subbasins of Cameron Highlands region of Peninsular Malaysia are provided. Further studies are needed on a large number of channel networks of distinct sizes and topologies to understand the relationships of these new exponents with other scaling exponents that define the scaling structure of river networks.

Citation: Tay, L. T., B. S. D. Sagar, and H. T. Chuah (2006), Allometric relationships between traveltime channel networks, convex hulls, and convexity measures, *Water Resour. Res.*, *42*, W06502, doi:10.1029/2005WR004092.

1. Introduction

[2] In geomorphic analysis, shape is crucial. The topology and geometry of networks play important role in understanding various watershed and geomorphic processes. Morphometry, fractal and allometric scaling analyses of such networks provide various characteristics in a quantitative manner [*Horton*, 1945; *Rodriguez-Iturbe and Rinaldo*, 1997; *Turcotte*, 1997; *Rigon et al.*, 1996; *Rinaldo et al.*, 1998; *Sagar et al.*, 1998, 2001; *Maritan et al.*, 2002; *Sagar and Tien*, 2004; *Sagar and Chockalingam*, 2004; *Chockalingam and Sagar*, 2005]. Existing popular scaling coefficients are directly measurable by defining topological aggregation, structure and length of drainage pattern, elongation, and general shape of the drainage basin [*Rinaldo et al.*, 1998]. The well-defined ranges of these scaling exponents reported as h, ξ, H, and β that realistic river networks possess are 0.53–0.60, 0.65–0.90, 0.70–1.00, and 0.41–0.46 respectively [*Rinaldo et al.*, 1998]. Basin processes are characterized by geomorphic width functions, and random cascade models that are based on network links and contributing areas [*Marani et al.*, 1991; *Gupta and Waymire*, 1993; *Marani et al.*, 1994; *Veneziano et al.*, 2000]. The general geometry and the diverging angles between the channel networks do not play a major role in such a characterization of basin processes. We demonstrate here the importance of the channel-network-dependent measures through considering a basin with typical topology and geometry of channel organization. These two important features represent topology-based network (which we call a minimum but contains highly significant morphological information), and geometry-based watershed boundary, respectively. The spatial organization of networks depends on contour geometry. Furthermore, the spatial organization of channel network patterns determines the basin processes, and one can reconstruct the basin with proper characteristics. This reconstruction will have several implications related to the geomorphic width function. When reconstructing the basin from the channel network, we apply a stepwise procedure. Figure 1 can be considered as the initial stage of the transformation of the channel network (nonconvex set) to the basin (convex set). A convex hull of a nonconvex set, is defined as the region within a boundary along the path taken by a tight rubber ring when it is warped around the nonconvex object (e.g., Figures 1a [*Turcotte et al.* 1998] and 1b). The channel network contains crucial information about a basin, or a convex hull.

[3] To have a better understanding of the basic formalism, the principles involved in generation of traveltime networks and construction of the corresponding convex hulls are explained in three-step procedure as follows.

[4] 1. Consider the branched river networks (tree-like networks) with a stationary outlet, lit the fire at all the extremities of river source and allow the fire to propagate uniformly toward outlet. As a result, the network subset would be burnt uniformly after periodic time intervals and these subsets after progressive levels of burning would be made union to visualize a network akin to the one shown in Figure 2a. The networks are pruned downward from ex-

[1]Faculty of Engineering, Cyberjaya Campus, Multimedia University, Cyberjaya, Selangor, Malaysia.
[2]Faculty of Engineering and Technology, Melaka Campus, Multimedia University, Bukit Beruang, Melaka, Malaysia.

0043-1397/06/2005WR004092$09.00

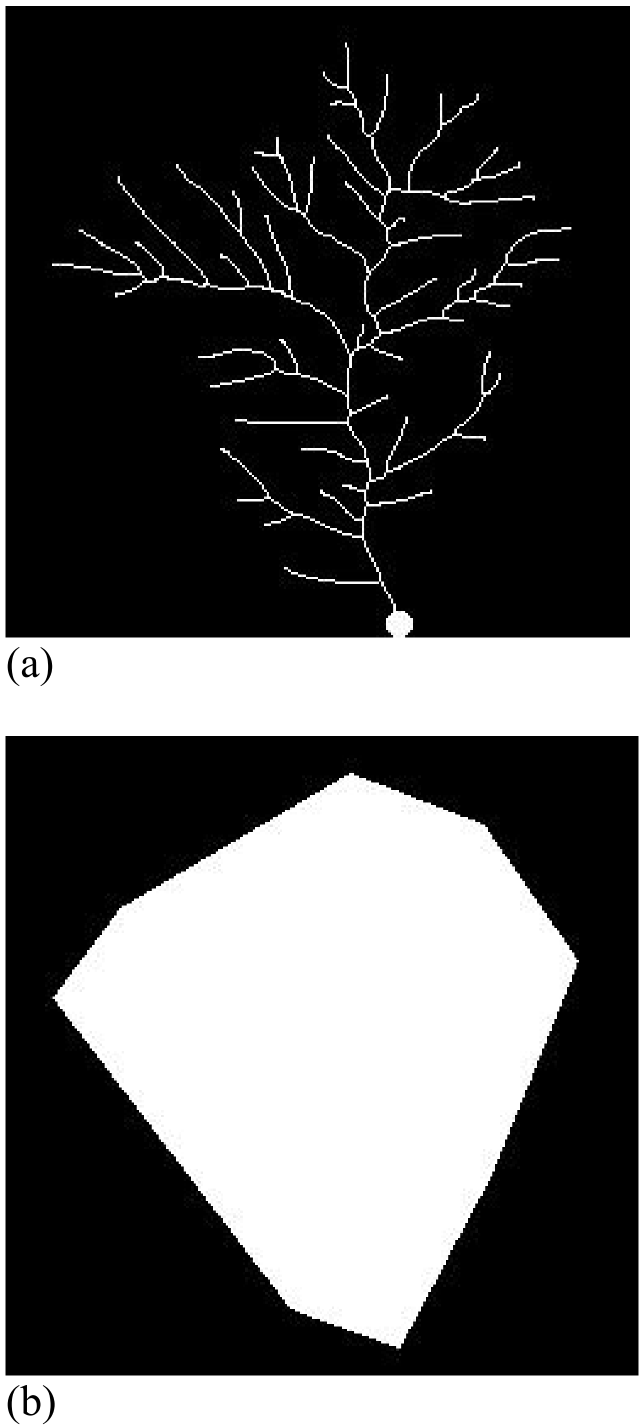

Figure 1. (a) An example of fourth-order channel network (nonconvex set) and (b) its convex hull. A stationary outlet is shown as a round dot in Figure 1a.

tremities (source points) to outlet by following the steepest descent (see Appendix A for mathematical approach to generate traveltime channel networks).

[5] 2. Convex hulls of the sequentially pruned networks are constructed (Appendix A).

[6] 3. Areas of the convex hulls are then plotted as function of lengths of the sequentially pruned networks. The area occupied by the nonconvex network, divided by the area of the corresponding convex hull gives the convexity measure function $CM(S)$.

[7] The details of this three-step procedure are given in sections 2, 3, and Appendix A. In summary, nonconvex and convex sets associated with pruned channel networks and

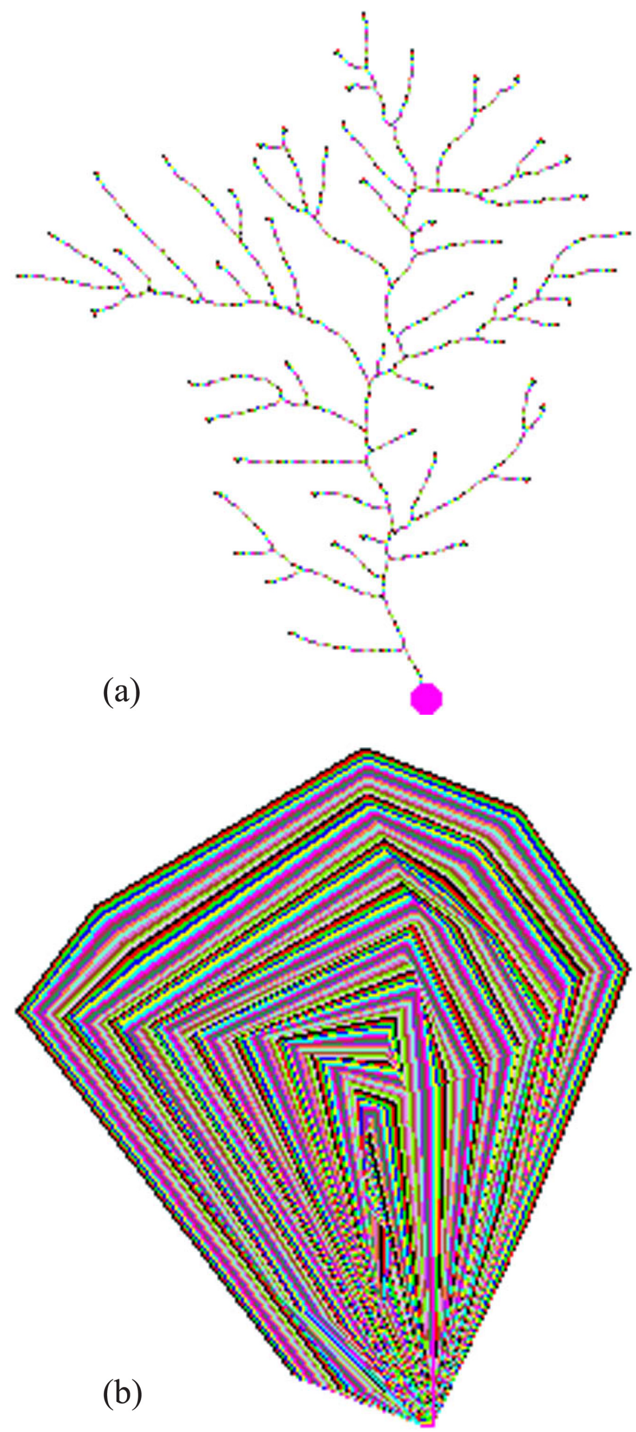

Figure 2. (a) Color-coded traveltime network pruned iteratively until it reaches the outlet and (b) color-coded union of convex hulls of networks pruned to different degrees. Figures S1a and S1b in the auxiliary material may be referred to for sequentially generated traveltime networks and their corresponding convex hulls.

their corresponding convex hulls, respectively, can be iteratively computed. Convex hulls of a sequentially and conditionally pruned network, in other words traveltime network that has a stationary-closed base, are noteworthy indicators of channel network morphology.

[8] The paper is organized as follows: We explain the methodology in section 2. In section 3, computation of convexity measures is provided, followed by section 4 depicting the derived results on a model channel network and certain realistic networks. Besides, the discussion of the results is presented. In section 5, conclusions are drawn and further research is called for. Basic morphological transformations and a mathematically viable procedure to generate traveltime networks and further to construct convex hull of each traveltime network are provided in Appendix A.

2. Methodology of Channel Network Decomposition and Convex Hull Construction

[9] Loopless channel network is decomposed into N channel subsets, where outlet is the order N subset and the extremities of the channel network are the first level open-ended channel subsets (or source points). The complex morphological transformations are required to accomplish the pruning iteratively starting from the extremities toward the outlet point to further generate traveltime network sequence.

[10] Sequentially pruned network construction is done to decompose a channel connectivity network into channel subsets of several orders. The process imitates uniform fire propagation in a tree-like structure. If we lit fire at all tips of the twigs of a tree, and the fire is allowed to propagate at uniform speed toward the base of the trunk, the whole tree would be burnt after some time depending upon the shape and size of the tree. The portions that are burnt off at regularly increasing time intervals are considered as traveltime subsets of different orders $n = 1$ to N of the tree network. If we replace the tree network with a river network, and neglect the actual geographic length of the branches, one can decompose the river connectivity network into river network subsets ranging from $n = 1$ to N. First and Nth level subset(s), respectively, stand for open-ended tips and a stationary outlet point of the river network.

[11] After deleting the end pixels the stream network (S) would yield S_1, followed by S_2 and finally S_N, where S_N is the outlet point. Some properties of a stream network that is pruned by deleting end pixels are as follows: (1) $S = \bigcup_{n=0}^{N-1} (S_n - S_{n+1})$, (2) $S_N \subset S_{N-1} \subset \cdots \subset S_2 \subset S_1 \subset S_0 = S$, (3) S, S_1, S_2, $\cdots$, S_N obtained by iterative pruning.

[12] The detailed transformations are explained in Appendix A. The logic behind peeling off the extremities of the channel network iteratively is based on considerations of the time required for the fluid particle to reach the outlet. During the peeling process, one can encounter extinguishing points or bifurcation points. A channel path between two points, in realistic case, is not the shortest Pythagorean distance, but has some amount of tortuosity. Consequently, the time required for a water particle to reach the outlet would be more than the time required in case of a particle that flows along a straight path. If the traveltime required for water particles from all source points to reach the outlet is the same, this indicates symmetry of the network.

[13] Convex hull of sequentially pruned networks is the smallest convex set that contains all the points of the network. From a network pruned from its full size till it reaches the outlet, one can construct convex hulls for all possible networks in a decreasing form. These conditionally shrinking traveltime networks are denoted by S, S_1, S_2, $\cdots$, S_N (Appendix A). The smallest convex set that includes a channel network S (Figure 1a) (which is a nonconvex set) is called the convex hull of S (Figure 1b) and it is denoted by $C(S)$. The convex hull of a nonconvex set is the smallest-area convex set which encloses nonconvex object and it is the shape of a rubber band stretched around the nonconvex object. This convex hull is a useful morphological descriptor of a channel network S. We are interested in the $C(S_n)$ of sequentially pruned channel networks S_n.

[14] To generate convex hulls for these traveltime networks (Figure S1a in the auxiliary material)[1] we employ Quickhull algorithm [*Barber et al.*, 1996] and the basic steps involved in the algorithm are provided in Appendix A.

[15] The convex set containing all the points of S yields $C(S)$. The convex hulls (Figure S1b in the auxiliary material) of $S_n (n = 0, 1, 2, 3, \cdots, N)$ possess the property of:

$$C(S_n) = C(S_N) \subset C(S_{n-1}) \subset C(S_{n-2}) \subset \cdots \subset C(S_2) \subset C(S_1) \subset C(S).$$

3. Convexity Measures of Nonconvex Traveltime Channel Networks: Power Laws

[16] The convexity measure of a nonconvex shape [*Heijmans and Tuzikov*, 1998; *Zunic and Rosin*, 2004] is defined as the ratio between the areas of S_n and areas of $C(S_n)$. The convexity measure of a channel network is a number between 0 and 1. The values 0 and 1, respectively, are the minimum possible and maximum possible measures, the latter is attained if and only if S is convex. The rate of change in the areas of S_n is relatively slower than that of $C(S_n)$. In channel network, area of S_n is equivalent to the length of the network, $L(S_n)$. Hence the convexity measures of decreasing $L(S_n)$ and $A[C(S_n)]$ converge.

[17] When analyzing a model network, we found three new allometric relationships between the lengths of the traveltime sequential network, the area of convex hulls, and the corresponding convexity measures: $L(S_n) \sim [A(C(S_n))]^{\alpha}$, $CM(S_n) \sim \frac{1}{L(S_n)^{\sigma}}$ and $CM(S_n) \sim \frac{1}{A[C(S_n)]^{\lambda}}$.

4. Model Study, Results, and Discussion

[18] We consider a model network [*Turcotte et al.*, 1998] occupying 256x260 pixels (Figure 1a). By following the morphological pruning approach explained in Appendix A, we convert this network into a traveltime sequence network (Figures 2a and S1a). The corresponding convex hulls of the network that is pruned to different decreasing lengths are computed (Figures 2b and S1b). This network took 246 iterations to reach the outlet. These 246 traveltime network sequences and their corresponding convex hulls are coded

[1] Auxiliary material is available at ftp://ftp.agu.org/apend/wr/wr004092.

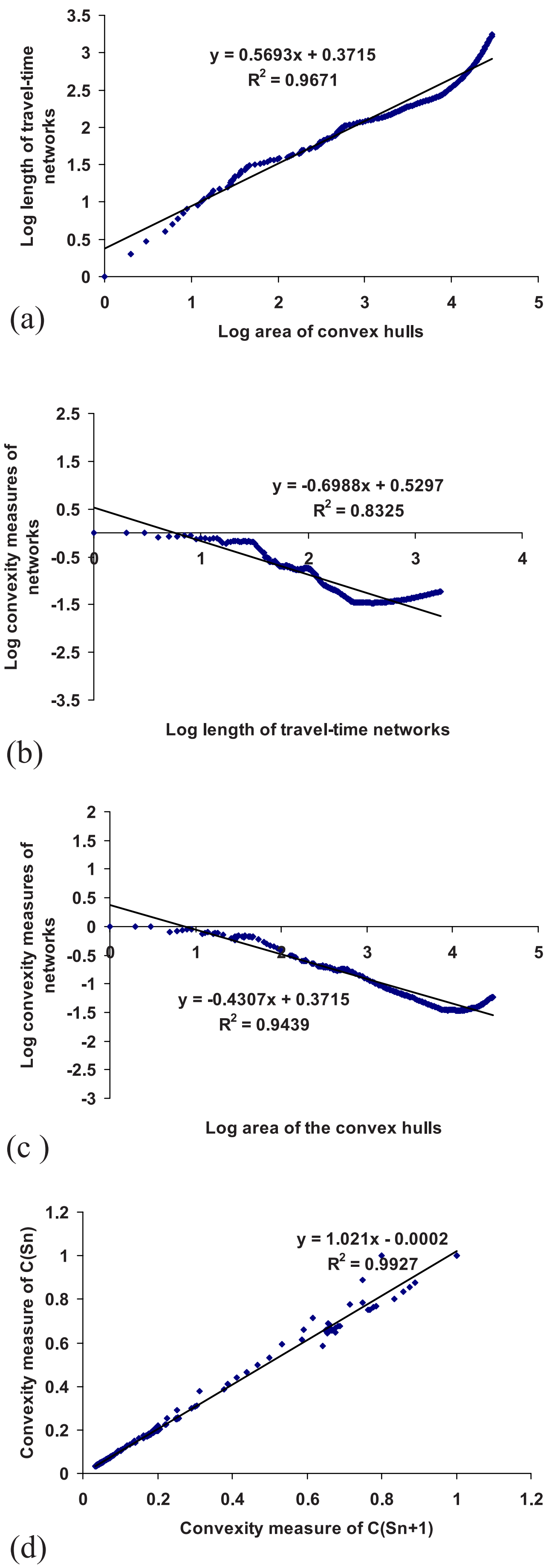

with colors for easier interpretation (Figures 2a and 2b). The network that is decomposed into traveltime sequences is color-coded as $S = \bigcup_{n=0}^{N-1} \bigcup_{i=n}^{255} (S_n - S_{n+1})^i$. Similarly, the convex hulls of the corresponding traveltime sequences are also color-coded as $C(S) = \bigcup_{n=0}^{N} \bigcup_{i=n}^{255} \{C(S_n) - C(S_{n+1})\}^i$. A nonconvex loopless network that is asymmetric possesses an asymmetric convex hull. Geometric similarity between all possible convex hulls of a decomposed traveltime sequence of networks indicates a symmetric network.

[19] Basic measures that include length of networks and areas of convex hulls were computed. From these basic measures, we compute convexity measures of traveltime networks. The upper limit of the convexity measure is attained when the length of the channel network is equal to the area of the convex hull (both being measured by number of pixels). One such example is the space-filling, Peano-curve-like network that has fractal Hausdorff dimension of 2 in the two-dimensional Euclidean space. This convexity measure of channel networks is similar to drainage density. Drainage density approaching 1 indicates that the channel network has become space filling. In this present model, we observe that the rate of change in the area of convex hulls is more rapid than the change in the length of the channel networks that are pruned iteratively toward the outlet. It would be interesting to find the connection of this measure with channel width function.

[20] Further allometric relationships between the lengths of the traveltime network sequences, areas of the corresponding convex hulls and their convexity measures are shown in Figures 3a–3c. We find a statistically significant scaling relationship for the model network in the form $L(S_n) \sim A[C(S_n)]^{0.57}$. Furthermore, when we plot the lengths of these traveltime networks and the areas of their corresponding convex hulls as functions of convexity measures, we arrive at new power law rules, such as $CM(S_n) \sim \frac{1}{L(S_n)^{0.7}}$ and $CM(S_n) \sim \frac{1}{A[C(S_n)]^{0.43}}$. These relationships are due to the fractal nature of the topological and geometric organization of the basin. In addition, we also consider channel networks from seven subbasins (Figure 4) extracted from digital elevation model of Cameron Highlands of Malaysia situated between 101°15′–101°20′E. longitudes and 4°31′–4°36′N. latitudes. By following the framework which is implemented on the model network, we derive results for these networks of seven subbasins (Table 1). Figure 3d shows the graphical relationship between the convexity measures of traveltime networks of successive discrete times n and $n + 1$. From Figure 3d, a linear relationship between convexity measures of successive traveltime networks is obvious.

[21] Bifurcation ratio (R_B), stream length ratio (R_L), Hack (h) and Hurst (H) exponents for the seven subbasins of Cameron Highlands are estimated (Table 1). Figure 5 shows basinwise exponent values. R_B and R_L range between 2.82

Figure 3. Crossplots between (a) lengths of the sequential pruned networks and the corresponding areas of convex hulls in logarithm scale, (b) lenghts and convexity measures in logarithm scale, (c) areas of convex hulls in logarithm scale, and (d) and convex measures in logarithm scale.

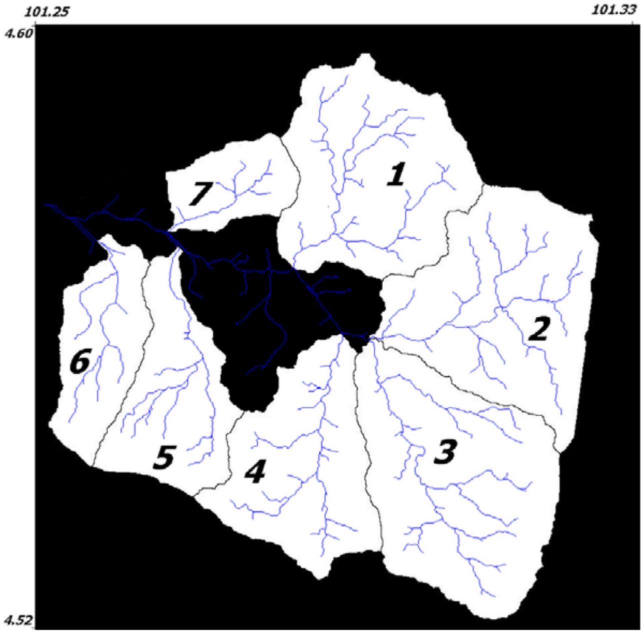

Figure 4. Channel networks derived for seven subbasins of Cameron Highlands of Malaysia.

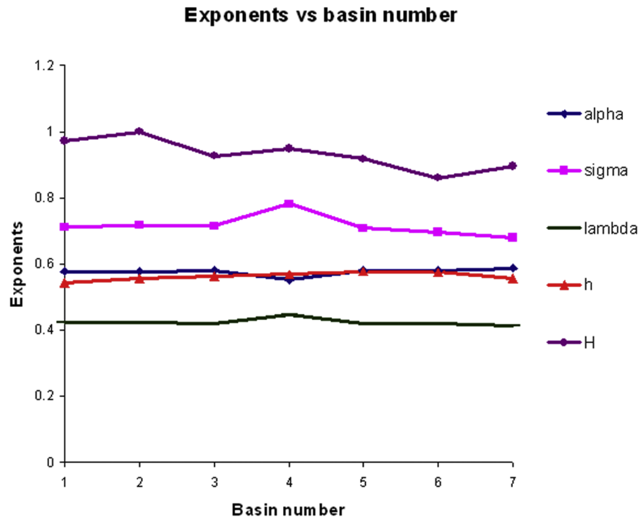

Figure 5. Basinwise exponents that include new exponents computed based on traveltime networks and their convex hulls and also other popular coefficients.

and 4.47, and 1.66 and 3.18, respectively. All the seven considered basins possess empirical values of *h*, which significantly differ from the Euclidean value of 0.5, as further evidence of their fractal nature. Hack exponents for these basins range between 0.541 and 0.577. Although the α and *h* values are similar, generally the α values are slightly higher. No significant relationship is observed between any of these proposed exponents and Hurst exponents. However, to substantiate this point and to relate with other two independent topological quantities such as bifurcation and stream length ratios, more sample networks are needed. To decide whether these allometric power laws are universal, a large number of synthetic and real channel networks with different topologies needs to be considered.

[22] It would be interesting by considering a large number of networks to explore the possible relations between the exponents derived based on traveltime networks and their convexity measures, and the existing popular scaling exponents. It would be interesting to know the following: (1) What would be the ranges of these exponents based on traveltime networks' convexity measures, between an elongated basin and radial basin? (2) what would be the rates of change in the convexity measures across traveltime networks in an elongated basin and in a circular basin? To address these points, one should use the framework adopted here to derive these exponents for basins with fixed values of $L_{\|}$ (longitudinal length) and varied values of $L_{\perp}$ (transverse length), with $L_{\perp} < L_{\|}$ to further relate with Hack and Hurst coefficients.

5. Conclusions

[23] In this paper, mathematical morphology transformations were used to generate a sequence of traveltime channel networks from the stationary network and Quickhull algorithm is used to construct convex hulls of the corresponding traveltime networks. The method can convert any branched loopless network into a sequence of traveltime networks and then into their convex hulls. The rate at which the channel network is pruned is related to the rate of change in the areas of the corresponding convex hulls of the traveltime networks. This relation can be expressed as a scale-independent power law. Also, it provides a set of convexity measures through which the lengths of sequential traveltime networks and their corresponding convex hulls can be related for a model network. Convexity measures of a dynamically shrinking traveltime network propagating toward its outlet provide new insights for geophysicists and geomorphologists to understand the channelization process. At a macroscopic level, these exponents complement with other existing popular scaling coefficients and can be used to identify commonly

Table 1. Allometric Power Laws Between Traveltime Channel Networks, Convex Hulls, and Convexity Measures for Model Network and Networks of Seven Basins of Cameron Highlands

Network	α (R^2)	σ (R^2)	λ (R^2)	R_B	R_L	*h*	H
Model	0.5693 (0.9671)	0.6988 (0.8325)	0.4307 (0.9439)	3.84	1.66		
Basin 1	0.5777 (0.9883)	0.7109 (0.9358)	0.4223 (0.9783)	3.60	2.21	0.5414	0.9714
Basin 2	0.5774 (0.9925)	0.7189 (0.9586)	0.4226 (0.9861)	4.35	2.25	0.5561	1
Basin 3	0.5799 (0.9934)	0.7131 (0.963)	0.4201 (0.9875)	3.31	2.39	0.5612	0.9256
Basin 4	0.5521 (0.9835)	0.7814 (0.92)	0.4479 (0.9752)	4.47	3.18	0.5671	0.9506
Basin 5	0.5798 (0.9905)	0.7083 (0.9469)	0.4202 (0.982)	3.31	2.16	0.5766	0.9162
Basin 6	0.5819 (0.9865)	0.6955 (0.925)	0.4181 (0.9743)	4.00	2.64	0.5746	0.8597
Basin 7	0.5885 (0.9887)	0.68 (0.9348)	0.4115 (0.9772)	2.82	2.39	0.5548	0.8950

(a)

0	0	0	0	0	0	0	0	0	0	0	0	0	0	0	0	0
0	0	0	1	0	0	0	0	0	0	0	0	0	0	0	0	0
0	0	1	1	1	0	0	1	0	0	0	0	1	0	0	0	0
0	1	1	1	1	1	1	1	1	1	1	1	1	1	1	0	0
0	0	1	1	1	0	0	1	0	0	1	0	0	0	0	0	0
0	0	0	1	0	0	0	0	0	0	0	0	0	0	0	0	0
0	0	0	0	0	0	0	0	0	0	0	0	0	0	0	0	0

(b)					(c)					(d)						
		0	1	0			1	0	1					1	1	1
B_1^1	=	1	**1**	1	B_2^1	=	0	O	0	B_1^1	∪	B_2^1	=	1	**1**	1
		0	1	0			1	0	1					1	1	1

(e)

1	*1*	0	*1*	0	*1*	*1*	*1*	*1*	*1*	*1*	*1*	*1*	*1*	*1*	*1*	*1*
1	0	0	0	0	0	0	*1*	0	*1*	*1*	*1*	0	*1*	0	*1*	*1*
0	0	0	**1**	0	0	0	0	0	0	0	0	0	0	0	0	0
1	0	**1**	**1**	**1**	0	0	***1***	0	0	*1*	0	*0*	*1*	0	*1*	*1*
0	0	0	**1**	0	0	0	0	0	0	0	0	0	0	0	0	0
0	0	0	0	0	0	0	0	0	0	0	0	0	0	0	0	0
1	0	0	0	0	0	0	*1*	0	0	*1*	0	*1*	*1*	*1*	*1*	*1*
1	*1*	0	*1*	0	*1*	*1*	*1*	*1*	*1*	*1*	*1*	*1*	*1*	*1*	*1*	*1*

(f)

0	0	0	0	0	0	0	0	0	0	0	0	0	0	0	0	0
0	0	0	0	0	0	0	0	0	0	0	0	0	0	0	0	0
0	0	0	0	0	0	0	0	0	0	0	0	0	0	0	0	0
0	0	0	0	0	0	0	***1***	0	0	0	0	0	0	0	0	0
0	0	0	0	0	0	0	0	0	0	0	0	0	0	0	0	0
0	0	0	0	0	0	0	0	0	0	0	0	0	0	0	0	0
0	0	0	0	0	0	0	0	0	0	0	0	0	0	0	0	0
0	0	0	0	0	0	0	0	0	0	0	0	0	0	0	0	0

Figure A1. (a) Numerals 1 and 0 respectively represent S and S^c, (b) B_1^k, (c) B_2^k, and (d) $B = B_1^k \cup B_2^k$. In Figures A1b–A1d the origin is the center of the 3 × 3 square. (e) Erosion of S by B_1^k (shown in bold) and erosion of S^c by B_2^k (shown in italics). (f) Eroded versions of S by ${B_1}^k$ intersect with the eroded version of S^c by B_2^k in one of the grids at (8, 4). Such intersecting portion results from the hit-or-miss transformation, in other words ($S * \{B\}$).

shared generic mechanisms in different river basins. An interesting open question is whether these scaling exponents hold good for a network in a basin and in networks in multitude of subbasins embedded within? To explore this question, further investigations are needed on a large number of channel networks of different sizes and topologies. A reasonable way to verify this is by hierarchically decomposing the basin into subbasins of various orders and apply the framework proposed here to explore the variations in the microscopic power law relationships, which would be useful to classify the subbasins. This would provide an insight to further explore links to find out what makes one subbasin different from the other within a large basin.

Appendix A

[24] In this Appendix we discuss technical details on the (1) generation of traveltime channel networks via pruning and (2) construction of convex hulls of corresponding traveltime networks. We first outline the basic morphological transformations required to prune the nonconvex channel network recursively.

[25] Let S and B in the two-dimensional Euclidean space represent a nonconvex channel connectivity network and a template with certain characteristic information such as size, shape, origin, and orientation [*Chockalingam and Sagar*, 2005], respectively. This template can be decomposed in several ways. Let S be a loopless network of one-pixel-wide channels. It is defined as the union of N channel subsets. The channel subset of order N is considered as an outlet (Figure 1). The extremities of the channel network are considered as first level open-ended channel subsets (or source points). The complex morphological transformations [*Serra*, 1982] are required to accomplish the first step of pruning extremities iteratively to further generate traveltime network sequence and they are explained in the following paragraph with the illustration provided schematically in Figure A1 [*Jang and Chin*, 1990]. This is named as hit-or-miss transformation, which is useful in detecting the exact pattern B_1 in the image S and is a subprocess involved in pruning.

$$B_1^1 = \begin{matrix} 1 & 0 & 0 \\ 0 & 1 & 0 \\ 0 & 0 & 0 \end{matrix} \quad B_1^2 = \begin{matrix} 0 & 0 & 1 \\ 0 & 1 & 0 \\ 0 & 0 & 0 \end{matrix} \quad B_1^3 = \begin{matrix} 0 & 0 & 0 \\ 0 & 1 & 0 \\ 0 & 0 & 1 \end{matrix} \quad B_1^4 = \begin{matrix} 0 & 0 & 0 \\ 0 & 1 & 0 \\ 1 & 0 & 0 \end{matrix}$$

$$B_1^5 = \begin{matrix} X & 1 & X \\ 0 & 1 & 0 \\ 0 & 0 & 0 \end{matrix} \quad B_1^6 = \begin{matrix} 0 & 0 & X \\ 0 & 1 & 1 \\ 0 & 0 & X \end{matrix} \quad B_1^7 = \begin{matrix} 0 & 0 & 0 \\ 0 & 1 & 0 \\ X & 1 & X \end{matrix} \quad B_1^8 = \begin{matrix} X & 0 & 0 \\ 1 & 1 & 0 \\ X & 0 & 0 \end{matrix}$$

$$B_2^1 = \begin{matrix} 0 & 1 & 1 \\ 1 & 0 & 1 \\ 1 & 1 & 1 \end{matrix} \quad B_2^2 = \begin{matrix} 1 & 1 & 0 \\ 1 & 0 & 1 \\ 1 & 1 & 1 \end{matrix} \quad B_2^3 = \begin{matrix} 1 & 1 & 1 \\ 1 & 0 & 1 \\ 1 & 1 & 0 \end{matrix} \quad B_2^4 = \begin{matrix} 1 & 1 & 1 \\ 1 & 0 & 1 \\ 0 & 1 & 1 \end{matrix}$$

$$B_2^5 = \begin{matrix} X & 0 & X \\ 1 & 0 & 1 \\ 1 & 1 & 1 \end{matrix} \quad B_2^6 = \begin{matrix} 1 & 1 & X \\ 1 & 0 & 0 \\ 1 & 1 & X \end{matrix} \quad B_2^7 = \begin{matrix} 1 & 1 & 1 \\ 1 & 0 & 1 \\ X & 0 & X \end{matrix} \quad B_2^8 = \begin{matrix} X & 1 & 1 \\ 0 & 0 & 1 \\ X & 1 & 1 \end{matrix}$$

Figure A2. Disjointed structuring templates in eight directions.

[26] In hit-or-miss transformation, morphological erosion [*Matheron*, 1975; *Serra*, 1982] is employed to shrink S and its complement, S^c. Erosion of S by B is defined as the set of points s such that the translated B_s is contained in S. This is expressed as

$$S \ominus \check{B} = \{s : B_s \subseteq S\} = \bigcap_{b \in \check{B}} S_b, \tag{A1}$$

where $\check{B}$ is a B rotated 180°. In the present case, $B = \check{B}$ as B rotated by 180° is equal to $\check{B}$. We employ this decomposition as follows: B is composed into two disjoint subsets B_1^1 and B_2^1 (e.g., Figures A1b–A1d), and the erosions of S by B_1^1 and S^c by B_2^1 are illustrated in Figure A1 [*Jang and Chin*, 1990]. In this schematic, S and S^c denote channel points with 1s and complement of channel network with 0s respectively. The union of B_1^1 and B_2^1 produces B which is the symmetric template about origin at center. Figures A1e and A1f illustrate respectively the logical union and intersection of eroded versions of S and S^c obtained with respect to B_1^1 and B_2^1. The intersection of S and S^c after eroding respectively by B_1^1 and B_2^1 is denoted by hit-or-miss transformation, ($S * \{B\}$). This transform is used in the channel network pruning process as described in the following section.

A1. Sequential Pruning of Networks

[27] To decompose a channel connectivity network into channel subsets of several orders, we adopt the morphological hit-or-miss-based thinning technique. The river connectivity networks are pruned iteratively and decomposed into river network subsets ranging from $n = 1$ to N. First and Nth level subset(s), respectively, stand for open-ended tips and a stationary outlet point of the river network. The implications of this decomposition procedure are described as follows.

[28] 1. Channel network (S) that possesses several orders of channels has a closed outlet (Figure 1a). A structuring template $\{B\}(= B_1^1 \cup B_2^1)$ that is disjointed into eight directions (Figure A2) is used to decompose the stream network subsets from n = 1 to N. First we find the intersecting portion of eroded S and eroded S^c, respectively by disjointed templates $\{B_1^k\}$ and $\{B_2^k\}$, $k = 1, 2, \cdots, 8$. Mathematically, $S * B = (S \ominus B_1^k) \cap (S^c \ominus B_2^k)$, where $B = B_1^k \cup B_2^k$ (Figures A1b–A1d).

[29] 2. By subtracting ($S * B$) from S, we get a pruned version of S, expressed as $S_1 = S \otimes \{B\}$, where $S \otimes \{B\} = S - (S * B))$, $S * B = (S \ominus B_1^k) \cap (S^c \ominus B_2^k)$, and $S \ominus B_1^k = \{x | (B_1^k)_x \subseteq S\}$.

[30] In other words, $S \otimes \{B\} = S - (S * \{B\})$, where $\{B\}$ is the sequence of $\{B\} = \{(B_1^1, B_1^2, \cdots, B_1^8), (B_2^1, B_2^2, \cdots, B_2^8)\}$ (Figure A2). This sequence of structuring elements consists of two structures, each of which is rotated by 90° for total eight elements. The "X"s in Figure A2 signify the "don't care" condition, in the sense that it does not matter whether the pixel in that location has a value of 0 or 1. $S \otimes \{B\} = ((\cdots((S \otimes B^1) \otimes B^2) \cdots) \otimes B^8)$. This equation explains the process of peeling of S in one pass with B^1, then peeling of the result in one pass with B^2 and so on until S is pruned in the last pass with B^8.

[31] 3. Applying this equation once, the first encountered open pixels of S would be burnt, and the traveltime network after deleting one end point in each source branches would yield S_1. Performing this equation on the S_1 once more would burn the open pixels of S_1, which is expressed as $S_1 \otimes \{B\} = S_1 - (S_1 * \{B\}) = S_2$. In other words, the intersection of eroded version of S_1 and S_1^c (that are eroded respectively by disjoint templates B_1^k and B_2^k, $k = 1, 2, \ldots, 8$) must be found to derive S_2. Further iteration of this equation would burn the end open pixels of S until a closed outlet is reached and the traveltime network after deleting n end points, S_n (where $n = 1$ to N) is saved.

[32] After deleting the end pixels the stream network (S) would yield S_1, next end pixels removing yield $S_1 \otimes \{B\} = S_2$, and finally $S_{N-1} \otimes \{B\} = S_N$, where S_N is the outlet point.

A2. Convex Hulls of Sequentially Pruned Networks

[33] From a network pruned from its full size till it reaches the outlet, one can construct convex hulls for all possible networks in a decreasing form. These conditionally shrinking traveltime networks are denoted by $S, S_1, S_2, \cdots, S_n$ and their corresponding convex hulls are denoted as $C(S), C(S_1), C(S_2), \ldots, C(S_n)$.

[34] To generate convex hulls for these traveltime networks (Figure S1a) we employ Quickhull algorithm [*Barber et al.*, 1996]. The basic steps (1–6) involved in this algorithm include the following.

[35] 1. Let the pruned network, S be a set of p points (p points represent all the pixels in the corresponding network).

[36] 2. The algorithm begins by building a convex hull from a small subset of the points in the set S.

[37] 3. Put all the points inside the convex hull into "inside set" and those outside into "outside set". Ignore those points in the "inside set".

[38] 4. Current convex hull has a few straight boundaries (the stretched rubber band). Assuming walls have been built along these boundaries and they are named as facets. Determine the facets (face) visible from every point in the "outside set". (A facet is considered to be visible from a point when it is possible to draw a straight line from the point to the facet without crossing other facets). Among the points in the "outside set" for each facet, search for the one, which is farthest from the hull.

[39] 5. Select point farthest from the hull from 4 and use it to update the hull.

[40] 6. Repeat the process recursively from step 3 to step 5 until all the points have been processed.

[41] The final convex set containing all the points of S yields $C(S)$. We employ this procedure to compute the convex hulls (Figure S1b) of S_n (n = 0, 1, 2, 3, $\cdots$, N).

[42] **Acknowledgments.** We are grateful to Gabor Korvin, Jayanth Banavar, Andrea Rinaldo and two anonymous reviewers for their encouragement, invaluable comments and suggestions to improve the presentation quality of the manuscript.

References

Barber, C. B., D. P. Dobkin, and H. T. Huhdanpaa (1996), The Quickhull algorithm for convex hulls, *ACM Trans. Math. Software*, *22*(4), 469–483.

Chockalingam, L., and B. S. D. Sagar (2005), Morphometry of network and non-network space of basins, *J. Geophys. Res.*, *110*, B08203, doi:10.1029/2005JB003641.

Gupta, V. K., and E. Waymire (1993), A statistical analysis of mesoscale rainfall as a random cascade, *J. Appl. Meteorol.*, *32*, 251–267.

Heijmans, H. J. A. M., and A. V. Tuzikov (1998), Similarity and symmetry measures for convex shapes using Minkowski addition, *IEEE Trans. Pattern Anal. Mach. Vision*, *20*, 980–993.

Horton, R. E. (1945), Erosional development of stream and their drainage basin: Hydrological approach to quantitative morphology, *Geol. Soc. Am. Bull.*, *56*, 275–370.

Jang, B. K., and R. T. Chin (1990), Analysis of thinning algorithms using mathematical morphology, *IEEE Trans. Pattern Anal. Mach. Intell.*, *12*, 541–551.

Marani, A., R. Rigon, and A. Rinaldo (1991), A note on fractal channel networks, *Water Resour. Res.*, *27*, 3041–3049.

Marani, M., A. Rinaldo, R. Rigon, and I. Rodriguez-Iturbe (1994), Geomorphological width functions and the random cascade, *Geophys. Res. Lett.*, *21*, 2123–2126.

Maritan, A., R. Rigon, J. R. Banavar, and A. Rinaldo (2002), Network allometry, *Geophys. Res. Lett.*, *29*(11), 1508, doi:10.1029/2001GL014533.

Matheron, G. (1975), *Random Sets and Integral Geometry*, John Wiley, Hoboken, N. J.

Rigon, R., I. Rodriguez-Iturbe, A. Giacometti, A. Maritan, D. Tarbotan, and A. Rinaldo (1996), On Hack's law, *Water Resour. Res.*, *32*, 3367–3374.

Rinaldo, A., I. Rodriguez-Iturbe, and R. Rigon (1998), Channel networks, *Annu. Rev. Earth Planet. Sci.*, *26*, 289–327.

Rodriguez-Iturbe, I., and A. Rinaldo (1997), *Fractal River Basins: Chance and Self-Organization*, Cambridge Univ. Press, New York.

Sagar, B. S. D., and L. Chockalingam (2004), Fractal dimension of non-network space of a catchment basin, *Geophys. Res. Lett.*, *31*, L12502, doi:10.1029/2004GL019749.

Sagar, B. S. D., and T. L. Tien (2004), Allometric power-law relationships of Hortonian fractal digital elevation model, *Geophys. Res. Lett.*, *31*, L06501, doi:10.1029/2003GL019093.

Sagar, B. S. D., C. Omoregie, and B. S. P. Rao (1998), Morphometric relations of fractal-skeletal based channel network model, *Discrete Dyn. Nature Soc.*, *2*(2), 77–92.

Sagar, B. S. D., D. Srinivas, and B. S. P. Rao (2001), Fractal skeletal based channel networks in a triangular initiator basin, *Fractals*, *9*, 429–437.

Serra, J. (1982), *Image Analysis and Mathematical Morphology*, Springer, New York.

Turcotte, D. L. (1997), *Fractals in Geology and Geophysics*, Cambridge Univ. Press, New York.

Turcotte, D. L., J. D. Pelletier, and W. I. Newman (1998), Networks with side branching in biology, *J. Theor. Biol.*, *193*, 577–592.

Veneziano, D., G. E. Moglen, P. Furcolo, and V. Iacobellis (2000), Stochastic model of the width function, *Water Resour. Res.*, *36*, 1143–1157.

Zunic, J., and P. L. Rosin (2004), A new convexity measure for polygons, *IEEE Trans. Pattern Anal. Mach. Vision*, *26*, 923–934.

H. T. Chuah and L. T. Tay, Faculty of Engineering, Cyberjaya Campus, Multimedia University, Jalan Multimedia, Cyberjaya 63100, Selangor, Malaysia. (htchuah@mmu.edu.my; lttay@mmu.edu.my)

B. S. D. Sagar, Faculty of Engineering and Technology, Melaka Campus, Multimedia University, Jalan Ayer Keroh Lama, Bukit Beruang 75450, Melaka, Malaysia. (bsdaya.sagar@mmu.edu.my)